

# Fingerprints of Dirac points in first-principles scanning tunneling spectra of graphene on a metal substrate

J. Sławińska<sup>1,2</sup> and I. Zasada<sup>2</sup>

<sup>1</sup>*Department of Theoretical Physics and Computer Science,  
University of Lodz, Pomorska 149/153, 90-236 Lodz, Poland*

<sup>2</sup>*Solid State Physics Department, University of Lodz, Pomorska 149/153, 90-236 Lodz, Poland*

Graphene physisorbed on a metal has its characteristic Dirac cones preserved in the band-structure, but the Fermi level of the system is shifted due to the interaction with the substrate. Based on density functional calculations with van der Waals corrections, we present a method to determine the position of the Dirac points with respect to the Fermi level from the measured scanning tunneling spectra. The analysis of local density of states profiles simulated for graphene on a metal surface allows to identify the Dirac points by linking the signatures in the calculated curves and the characteristic points in the band-structures. The positions of the dips in simulated differential tunneling spectra of graphene on a Cu(111) surface are in a close agreement with the experimental ones presented in the recent studies. It is demonstrated that including van der Waals interactions is essential for determining the electronic structure of graphene-metal interface in agreement with experimental findings.

PACS numbers: 73.22.Pr, 71.15.Mb, 68.37.Ef

The unique properties of graphene [1], such as its ultrathin geometry [2] and high carrier mobility [3] makes it a promising candidate for applications in future nanoelectronics, sensors and photonics [4, 5]. Making complex devices requires the production of large enough high-quality graphene sheets to achieve scalability and benefit from exceptional electronic properties observed in the flat domains of the monolayer sheets [6]. In practice, the large-area graphene has been grown epitaxially on transition metals [7, 8], especially the chemical vapor deposition (CVD) method has been developed to synthesize graphene on copper [9] and gold [10] substrates, although their catalyst's role is still not well understood [11]. Due to high-quality and transferability of the samples prepared on Cu surfaces, much theoretical [12–17] and experimental effort [18] has been devoted to shed the light on the mechanisms of graphene-metal interactions as well as on the modifications of its electronic properties. In particular, the doping effect [17] in physisorbed graphene has been widely studied both theoretically and experimentally by using a number of techniques, as for example density functional theory (DFT) and scanning tunneling microscopy (STM).

Scanning probe methods [19] have developed into a powerful tool for the determination of the structure of surfaces and interfaces, thus it is especially suitable for studies of graphene deposited on conductive substrates. The scanning tunneling spectroscopy (STS) mode allows to record the first derivative of the tunneling current with respect to the bias voltage which is the measure of the surface density of states at every arbitrarily fixed point. The electronic structure is probed locally [20], thus the presence of heterogeneity at different places on the surface or periodically repeated domains can be identified. Moreover, the information how the metal surface states

are modified by the adsorption of graphene sheet can be obtained after careful analysis.

According to early local density approximation (LDA)-based DFT studies [13] of a graphene/Cu(111) system, the physisorption leads to the change in the location of Dirac point, since the electrons are donated by a substrate to graphene (n-type doping of -0.17 eV). In a recent experimental study of graphene epitaxially grown on a Cu(111) surface the results of STS measurements are reported [18]. The dip in the presented STS profile (Fig.3C in Ref.[18]) at approximately -0.35 eV is associated with the Dirac point shifted below the Fermi level, which qualitatively confirms previous theoretical results. However, the interpretation of differential tunneling spectra is not straightforward due to the influence of the tip states [20]. Thus, as suggested in Ref.[18] only a combination of STS with a secondary experimental technique could give a direct evidence that a dip reflects the local density of states at the Dirac point of graphene. Angle-resolved photoemission spectroscopy (ARPES) could confirm the energy position of the Dirac point, however sufficiently large monocrystalline samples are required to find specific paths inside the Brillouin zone of the system. On the other hand, the new methods of Dirac point mapping have been proposed, such as following the gate-dependent position of adjacent dips in the tunable system [21] or analysis of Fourier transforms of STM maps revealing a linear dispersion relation for states above and below the Fermi energy [22]. They are, however, either not applicable for conductive substrate or at least hardly achievable without special equipment such as low temperature (LT) STM with lock-in detection. This indicates that linking theoretical predictions and experimental findings needs an approach independent of the limitations of measurement and preparation methods.

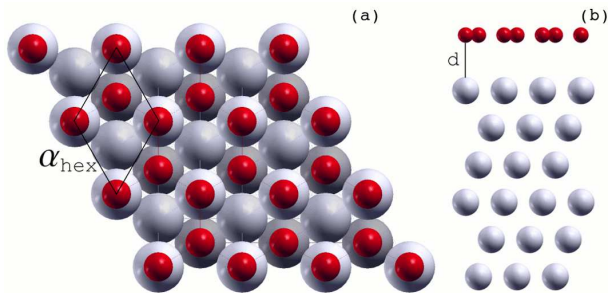


FIG. 1: (Color online) Top view (a) and side view (b) of adsorption geometry of graphene on a Cu(111) substrate. Carbon atoms are denoted as red (darker) balls, copper atoms as gray balls. Parallelogram defines the unit cell.

In this letter, we report on the first principles simulations of differential spectra that can be directly compared with measured  $dI/dV$  profiles of graphene on a metal surface. As DFT method provides the information about the band-structure, the dip in calculated LDOS above the surface can be unambiguously linked to the energy position of Dirac points in the dispersion relation. The example of graphene on a Cu(111) substrate has been carefully elaborated to test the presented method.

All DFT calculations have been performed using VASP package [23, 24] equipped with the projector augmented wave (PAW) method [25, 26] for electron-ion interactions. The exchange-correlation energy is calculated using the generalized gradient approximation within the Perdew, Burke and Ernzerhof (PBE) [27] parametrization scheme. Long-range dispersion corrections have been taken into account within a DFT-D2 approach of Grimme [28], as implemented in the latest version of VASP [29]. The pair interactions up to a radius of 12 Å have been included in the calculations and the global scaling factor  $s_6$  has been set to 0.75 due to the choice of the PBE functional. The dispersion coefficients  $C_6$  and van der Waals radii  $R_0$  for C and Cu atoms are defined in the code, according to the suggestion of Grimme [28]. The electronic wave functions have been expanded in a plane-wave basis set of 400 eV, while the electronic self-consistency criterion has been set to  $10^{-7}$  eV.

The (111) surface of Cu is simulated by a periodic slab geometry. Supercells containing six layers of metal and a graphene sheet adsorbed on top are separated by the vacuum thickness of at least 20 Å. The typical in-plane adsorption geometry is shown in Fig.1 (a). The graphene-metal interface is modeled by direct matching of a graphene's and a substrate's unit cells, although in the real systems the lattice-mismatch leads to the Moiré pattern on the surface. This artificially generated strain tends to affect the surface relaxation and the electronic properties, which was discussed in Ref. [17]. Thus, we have performed calculations for both configurations: with the in-plane lattice parameter  $\alpha_{\text{hex}}$  equal to the

PBE+D2-optimized value for graphene 2.466 Å as well as with the lattice constant adapted to that of a metal (two cases were considered: PBE+D2 optimized  $\alpha_{\text{hex}} = 2.524$  Å and an experimental value of 2.56 Å). There exist also three inequivalent stacking orders of graphene and Cu layers. The carbon atoms can lie above metal atoms in layers 1 and 3 (known as the top-fcc configuration, see Fig.1), 1 and 2 (a top-hcp) or 2 and 3 (a hcp-fcc). The previous LDA study [14] identified the top-fcc configuration as the most stable one, which was also confirmed by the present vdW calculations. During all structure relaxations the copper in top two layers as well as all carbon atoms have been allowed to move. Total energies were converged to within  $10^{-6}$  with respect to the ionic steps.

The problem of accurate Brillouin zone sampling is of particular importance for simulations of local density of states above the surface. The simulations of STM images is not computationally demanding, but the resolution of the calculated STS profiles is determined by the accuracy of the band-structure maps. For example, the identification of the onset of a noble metal surface requires at least one k-point every few meV for a specific band which means a few thousands of k-points in the Brillouin zone [30]. During the relaxation and the self-consistent run we applied the tetrahedron scheme [31] and the  $\Gamma$ -centered  $36 \times 36 \times 1$  k-point mesh, whereas in the non-self-consistent final calculations, a dense map of more than 10000 k-points and the Gaussian smearing of width  $\sigma = 0.05$  eV has been used.

The Tersoff-Hamann model of tunneling, due to its simplicity and qualitative reliability, is implemented in VASP as well as nearly every other DFT code to make simulations of pseudo-STM topography images. In this approach the tunneling current is proportional to the local density of states at the position of the STM tip [19]:

$$I(\mathbf{R}) \sim \sum_{\substack{E_n < E_F \\ E_n > E_F - eV_{\text{bias}}}} |\psi(\mathbf{R}, E_n)|^2$$

Provided that the k-points mesh is sufficiently fine, the reliable pseudo-STs profiles can be obtained by an evaluation of the constant-height charge images for several values of bias voltage followed by their numerical differentiation. The local density of states is automatically calculated in every single point above the surface and the choice of a spectrum in the particular position could correspond to the STS data taken under open loop conditions at the fixed point.

The local densities of states of a clean perfect Cu(111) surface are shown in Fig. 2 (a). We have evaluated the spectra for all three considered choices of the in-plane lattice parameter  $\alpha_{\text{hex}}$ . Their overall shape is similar to those presented in the previous theoretical studies [30, 32] as well as to the data obtained in a number of experiments [33, 34]. The step-shaped onsets of the surface state can be easily observed at bias voltages  $U_1 = -700$

mV,  $U_2 = -440$  mV and  $U_3 = -280$  mV for the values of lattice constants  $\alpha_{\text{hex}}^1 = 2.466$ ,  $\alpha_{\text{hex}}^2 = 2.524$  and  $\alpha_{\text{hex}}^3 = 2.56$  Å, respectively. It should be noted that the oscillations present in the profiles originate from a discrete k-points mesh. According to the discussion presented in Ref. [30], the signature of a surface electronic structure should be very sensitive to the choice of the lattice constant. Indeed, the experimental position of the surface state is reproduced only for a value of the lattice constant  $\alpha_{\text{hex}}^2$  optimized within the PBE+D2 approach. This appears to be in contrast with previous theoretical results based on a Perdew-Wang (PW91) parametrization, where setting the  $\alpha_{\text{hex}}$  to an experimental value was needed to obtain the quantitatively correct data. The discrepancies seem to be caused by using of a different parametrization approach and will be widely discussed in a separate study. The problem of the surface onset shift is especially important for modeling the graphene-metal interface where adjusting the substrate's lattice constant to graphene is usually required [17]. It means that a correct theoretical determination of subtle features such as experimentally observed suppression of a Cu(111) surface state in the presence of graphene [18] could be hardly achievable within a  $1 \times 1$  supercell approach.

The bonding of graphene to a copper surface is rather weak and the characteristic Dirac cones are nearly preserved in the band-structure. Both LDA [35] and the present DFT-D2 calculations predict a tiny band-gap of the order of 10 meV in the case of the matched unit cells, but in a real incommensurate interface this gap should disappear. The physisorption of graphene on a Cu(111) substrate causes a Fermi level shift upward [13]. In Fig.2 (b) we present the energy dispersion relation of graphene-Cu(111) system for a value of  $\alpha_{\text{hex}} = 2.466$  Å. The similar band-structures have been obtained for other values of the lattice constant, i.e. 2.524 Å and 2.56 Å. The optimized adsorption distances are about 3.06 Å 2.98 Å and 2.88 Å, respectively. We define the doping level as  $\Delta E_F = E_D - E_F$ , i.e. a difference between Dirac point energy and a Fermi level. The values of doping levels are equal to -0.427 eV, -0.584 eV and -0.686 eV for the considered lattice parameters, respectively. Since DFT-D2 tends to slightly underestimate the adsorption distances [36], also the calculated doping level can be slightly below the measured values.

The STM experiment of graphene on a Cu(111) substrate revealed a Moiré pattern present on the surface [18]. It means that the length of graphene bonds is preserved, which seems to be common for all weakly binding systems. Moreover, it has been previously demonstrated for a similar system, that the most reliable values of doping are obtained when a unit cell is adjusted to graphene's lattice constant. For example, in case of graphene - gold interface, stretching of bonds leads to the value of doping which is in disagreement with the experimental data [37]. The choice of  $\alpha_{\text{hex}} = 2.466$  Å should then lead to

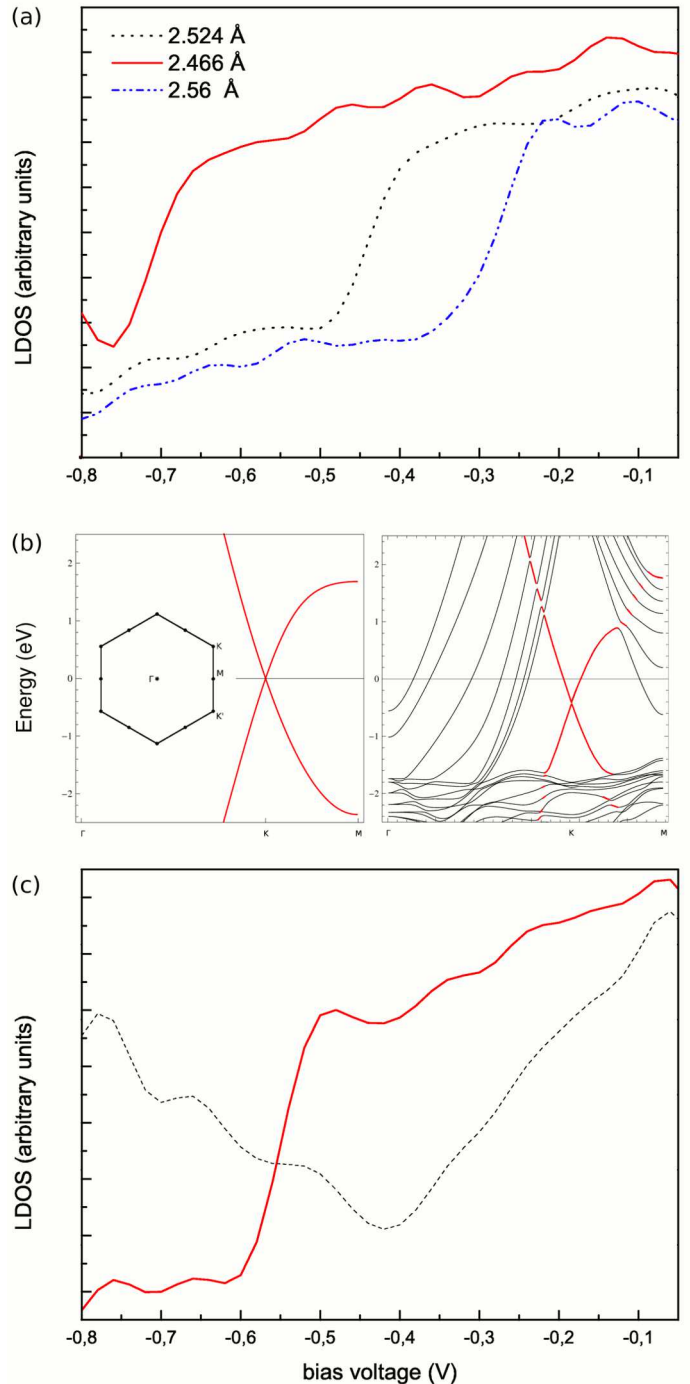


FIG. 2: (Color online) (a) The simulated LDOS spectra of a clean Cu(111) surface for different choices of the in-plane lattice parameter  $\alpha_{\text{hex}}$  (b) Left panel: The band-structure of freestanding graphene. The inset shows a Brillouin zone with the  $\Gamma$ , K, and M high-symmetry points. Right panel: The electronic structure of graphene on Cu(111). (c) The calculated LDOS profile above the surface of a graphene - Cu(111) system for a sample-tip distance larger than 2 Å (solid line) and equal to about 1 Å (dashed line). The parameter  $\alpha_{\text{hex}}$  has been set to 2.466 Å. The zero energy is at a Fermi level.

the most accurate description of the graphene's electronic properties.

In Fig. 2(c) we present a LDOS spectrum for a graphene-Cu(111) interface simulated with the  $\alpha_{\text{hex}}=2.466 \text{ \AA}$  (solid line). Since the position of the Dirac point is known from the band-structure (see Fig. 2 (b)), we can directly map it onto an STS profile. It means that a dip at  $-0.427 \text{ eV}$  in the spectrum (Fig. 2 (c), solid line) can be associated with the Dirac point in the energy dispersion, which provides an unambiguous link between experimental STS profiles and the calculated band-structures. In this light, the local minimum observed at  $-0.35 \text{ eV}$  in the spectrum (Fig. 3C in Ref. [18]) should be indeed interpreted as a signature of a Dirac point. The measured value of doping is quite close to the one predicted in the present study. The difference of about  $80 \text{ meV}$  might be explained by the effect of phonon-mediated inelastic tunneling as recently discussed in Ref. [21]. This phenomenon could cause a systematic shift of a Dirac point dip toward the Fermi level by about few tens of meV. Another reason for a doping level shift may be connected with the adsorption distance underestimated in the DFT-D2 approach.

Despite the oscillations related to the finite resolution of the spectrum presented in Fig. 2 (c), a Dirac point dip can be still easily recognized. However, if the profile is evaluated using the minimal required k-points mesh the Dirac point can be hardly identified. One may additionally confirm its location by decreasing the tip-sample distance, i.e. approaching to the surface (Fig. 2 (c), dashed line). At the distances of the order of  $1 \text{ \AA}$  above the surface, the graphene states dominate in the spectrum and the minimum can be unambiguously recognized.

It should be also noted that the onset of a Cu(111) surface state after the deposition of graphene (Fig. 2 (c), solid line) is shifted toward the Fermi level with respect to the position predicted in the calculations for a clean surface done using the same lattice-constant parameter  $\alpha_{\text{hex}}=2.466 \text{ \AA}$  (Fig. 2 (a), solid line). It appears to be connected with the changes in the work function upon adsorption of the carbon atoms.

In summary, we have performed DFT-D2 calculations for graphene-Cu(111) system and evaluated the corresponding LDOS spectra above the surface. The fingerprints of Dirac points present in the band-structure are easily recognized in the simulated STS profiles which enables a straightforward comparison of theoretical and experimental data. The doping predicted in the present study is in better agreement with the measured value than the previous LDA results. It provides the evidence that vdW forces are responsible for the properties of graphene-metal interfaces.

We thank Z. Klusek and P. Dabrowski for helpful discussions. This work is financially supported by Polish Ministry of Science and Higher Education in the frame of Grant No. N N202 204737. One of us (J.S.) ac-

knowledges support from the European Social Fund implemented under the Human Capital Operational Programme (POKL), Project: D-RIM. Figure 1 was prepared using the XCRYSDEN program. [38]

- 
- [1] A. H. C. Neto, F. Guinea, N. M. R. Peres, K. S. Novoselov, and A. K. Geim, *Rev. Mod. Phys.* **81**, 109 (2009).
  - [2] K. S. Novoselov, A. K. Geim, S. V. Morozov, D. Jiang, Y. Zhang, S. V. Dubonos, I. V. Grigorieva, and A. A. Firsov, *Science* **306**, 666 (2004).
  - [3] F. Schwierz, *Nat Nano* **5**, 487 (2010).
  - [4] F. Xia, D. B. Farmer, Y.-m. Lin, and P. Avouris, *Nano Lett.* **10**, 715 (2010).
  - [5] Q. Bao, H. Zhang, B. Wang, Z. Ni, C. H. Y. X. Lim, Y. Wang, D. Y. Tang, and K. P. Loh, *Nat Photon* (2011).
  - [6] D. Stradi, S. Barja, C. Díaz, M. Garnica, B. Borca, J. J. Hinarejos, D. Sánchez-Portal, M. Alcami, A. Arnau, A. L. Vázquez de Parga, R. Miranda, and F. Martín, *Phys. Rev. Lett.* **106**, 186102 (2011).
  - [7] A. T. N'Diaye, S. Bleikamp, P. J. Feibelman, and T. Michely, *Phys. Rev. Lett.* **97**, 215501 (2006).
  - [8] A. L. Vázquez de Parga, F. Calleja, B. Borca, M. C. G. Passeggi, J. J. Hinarejos, F. Guinea, and R. Miranda, *Phys. Rev. Lett.* **100**, 056807 (2008).
  - [9] X. Li, W. Cai, J. An, S. Kim, J. Nah, D. Yang, R. Piner, A. Velamakanni, I. Jung, E. Tutuc, S. K. Banerjee, L. Colombo, and R. S. Ruoff, *Science* **324**, 1312 (2009).
  - [10] T. Oznuluer, E. Pince, E. O. Polat, O. Balci, O. Salihoglu, and C. Kocabas, *Applied Physics Letters* **98**, 183101 (2011).
  - [11] W. Liu, H. Li, C. Xu, Y. Khatami, and K. Banerjee, *Carbon In Press, Accepted Manuscript*, (2011), ISSN 0008-6223.
  - [12] G. Giovannetti, P. A. Khomyakov, G. Brocks, V. M. Karpan, J. van den Brink, and P. J. Kelly, *Phys. Rev. Lett.* **101**, 026803 (Jul 2008).
  - [13] P. A. Khomyakov, G. Giovannetti, P. C. Rusu, G. Brocks, J. van den Brink, and P. J. Kelly, *Phys. Rev. B* **79**, 195425 (May 2009).
  - [14] Z. Xu and M. J. Buehler, *Journal of Physics: Condensed Matter* **22**, 485301 (2010).
  - [15] M. Vanin, J. J. Mortensen, A. K. Kelkkanen, J. M. Garcia-Lastra, K. S. Thygesen, and K. W. Jacobsen, *Phys. Rev. B* **81**, 081408 (2010).
  - [16] I. Hamada and M. Otani, *Phys. Rev. B* **82**, 153412 (Oct 2010).
  - [17] J. Sławińska, P. Dabrowski, and I. Zasada, *Phys. Rev. B* **83**, 245429 (2011).
  - [18] L. Gao, J. R. Guest, and N. P. Guisinger, *Nano Letters* **10**, 3512 (2010).
  - [19] W. A. Hofer, *Progress in Surface Science* **71**, 147 (2003).
  - [20] N. Nicoara, E. Romo-Ángel, J. M. Gázquez-Rodríguez, J. A. Martín-Gago, and J. M. Asua, *Organic Electronics* **7**, 287 (2006).
  - [21] Y. Zhang, V. W. Brar, F. Wang, C. Girit, Y. Yayon, M. Panlasigui, A. Zettl, and M. F. Crommie, *Nat Phys* **4**, 627 (2008).
  - [22] Y. Zhang, V. W. Brar, C. Girit, A. Zettl, and M. F. Crommie, *Nat Phys* **5**, 722 (2009).

- [23] G. Kresse and J. Furthmüller, Computational Materials Science **6**, 15 (1996).
- [24] G. Kresse and J. Furthmüller, Phys. Rev. B **54**, 11169 (1996).
- [25] P. E. Blöchl, Phys. Rev. B **50**, 17953 (1994).
- [26] G. Kresse and D. Joubert, Phys. Rev. B **59**, 1758 (1999).
- [27] J. P. Perdew, K. Burke, and M. Ernzerhof, Phys. Rev. Lett. **77**, 3865 (1996).
- [28] S. Grimme, J Comput Chem **27**, 1787 (2006).
- [29] T. Bucko, J. Hafner, S. Lebegue, and J. G. Angyan, The Journal of Physical Chemistry A **114**, 11814 (2010).
- [30] W. A. Hofer and A. Garcia-Lekue, Phys. Rev. B **71**, 085401 (2005).
- [31] P. E. Blöchl, O. Jepsen, and O. K. Andersen, Phys. Rev. B **49**, 16223 (1994).
- [32] S. Lounis, P. Mavropoulos, P. H. Dederichs, and S. Blügel, Phys. Rev. B **73**, 195421 (2006).
- [33] J. Kliewer, R. Berndt, E. V. Chulkov, V. M. Silkin, P. M. Echenique, and S. Crampin, Science **288**, 1399 (2000).
- [34] I. Jeon, H. Yang, S.-H. Lee, J. Heo, D. H. Seo, J. Shin, U.-I. Chung, Z. G. Kim, H.-J. Chung, and S. Seo, ACS Nano **5**, 1915 (2011).
- [35] G. Giovannetti, P. A. Khomyakov, G. Brocks, P. J. Kelly, and J. van den Brink, Phys. Rev. B **76**, 073103 (2007).
- [36] K. Tonigold and A. Gross, The Journal of Chemical Physics **132**, 224701 (2010).
- [37] Z. Klusek, P. Dabrowski, P. Kowalczyk, W. Kozłowski, W. Olejniczak, P. Blake, M. Szybowicz, and T. Runka, Applied Physics Letters **95**, 113114 (2009).
- [38] A. Kokalj, Comput. Mater. Sci. **28**, 155 (2003), <http://www.xcrysden.org/>.